2006

# Aeolian-fluvial interaction: evidence for Late Quaternary channel change and wind-rift linear dune formation in the northwestern Simpson Desert, Australia

Gerald C. Nanson
*University of Wollongong*, gnanson@uow.edu.au

Brian G. Jones
*University of Wollongong*, briangj@uow.edu.au

David M. Price
*University of Wollongong*, dprice@uow.edu.au

Tim Pietsch
*Griffith University*

C Bristow
*University of London*

*See next page for additional authors*

# Aeolian-fluvial interaction: evidence for Late Quaternary channel change and wind-rift linear dune formation in the northwestern Simpson Desert, Australia


## Abstract

In central Australia the most easterly extent of the MacDonnell Ranges borders the northwestern Simpson Desert where widely spaced strike ridges intercept the regional linear dunefield. Topographic basins have disrupted regional drainage lines and isolated dune sets from the main dunefield. In the western part of Camel Flat basin large, red coloured linear dunes of fine sand, ~ 74 ka and older, are oriented almost due north. Through gaps in the ranges the Todd River traversed the eastern part of the basin until ~25 ka when it apparently avulsed ~25 km eastwards to its present position. Subsequently, linear dunes, smaller, lighter in colour and coarser-textured, prograded onto the abandoned floodplain in the basin at rates of about 0.25-0.35 m a-1 and with orientations 20o further to the west than the older dunes. This new alignment suggests a latitudinal wind-whorl shift of some 160 km or 1.5o since the Last Glacial Maximum. Where dunes free of fluvial interference ramp onto the southern footslopes of the bedrock ridges they yield ages of at least ~65 ka, similar to the red dunes in the western part of the basin. These results highlight the difficulty of separating or interrelating the impacts of climate change, catastrophic flooding and aeolian damming as possible causes of Quaternary landscape change in the MacDonnell Ranges.



## Keywords

Aeolian, fluvial, interaction, evidence, for, Late, Quaternary, channel, change, wind, rift, linear, dune, formation, northwestern, Simpson, Desert, Australia, GeoQUEST

## Disciplines

Life Sciences | Physical Sciences and Mathematics | Social and Behavioral Sciences

## Publication Details

Hollands, C. B., Nanson, G. C., Jones, B. G., Price, D. M., Pietsch, T. & Bristow, C. S. (2006). Aeolian-fluvial interaction: evidence for Late Quaternary channel change and wind-rift linear dune formation in the northwestern Simpson Desert, Australia. Quaternary Science Reviews, 25 (1-2), 142-162.



## Authors

Gerald C. Nanson, Brian G. Jones, David M. Price, Tim Pietsch, C Bristow, and Cameron B. Hollands

**(This copy last revised by CBH on 6/2/04)**

**(Prepared for Quaternary Science Reviews)**

# Aeolian-Fluvial Interaction: Late Quaternary Channel Change and Dune Formation in the Simpson Desert near Alice Springs, Australia

**Cameron B. Hollands, Gerald C. Nanson** (gnanson@uow.edu.au)**, Brian G. Jones, David M. Price and Timothy J. Pietsch**

**School of Earth and Environmental Science, University of Wollongong, New South Wales, Australia**

**Charlie S. Bristow**

**School of Earth Sciences, Birkbeck College, University of London, Malet Street. London, WC1E 7HX, UK**

## ABSTRACT

In central Australia the most easterly extent of the MacDonnell Ranges borders the northwestern Simpson Desert where widely spaced strike ridges intercept the regional linear dunefield. Topographic basins have disrupted regional drainage lines and isolated dune sets from the main dunefield. In the western part of Camel Flat basin large, red coloured linear dunes of fine sand, ~ 74 ka and older, are oriented almost due north. Through gaps in the ranges the Todd River traversed the eastern part of the basin until ~25 ka when it apparently avulsed ~25 km eastwards to its present position. Subsequently, linear dunes, smaller, lighter in colour and coarser-textured, prograded onto the abandoned floodplain in the basin at rates of about 0.25-0.35 m $a^{-1}$ and with orientations $20^{o}$ further to the west than the older dunes. This new alignment suggests a latitudinal wind-whorl shift of some 160 km or $1.5^{o}$ since the Last Glacial Maximum. Where dunes free of fluvial interference ramp onto the southern footslopes of the bedrock ridges they yield ages of at least ~65 ka, similar to the red dunes in the western part of the basin. These results highlight the difficulty of separating or interrelating the impacts of climate change, catastrophic flooding and aeolian damming as possible causes of Quaternary landscape change in the MacDonnell Ranges.

**Key words:** Simpson Desert, MacDonnell Ranges, water gaps, aeolian-fluvial interaction, wind regimes, channel avulsion, luminescence dating, ground penetrating radar.

## INTRODUCTION

The Simpson Desert represents the eastern portion of a whorl of mostly linear and generally well vegetated dunes that dominate continental Australia (Brookfield, 1970). This whorl was originally mapped by King (1960) and then in more detail by Wasson *et al.* (1988). Linear dunes are Australia's most extensive landform covering 40% of the continent (Wasson *et al.*, 1988), yet only a limited amount is known about their chronology and interaction with adjacent river systems and ranges. This paper uses field-surveying, thermoluminescence (TL) and optically stimulated luminescence (OSL) dating, grain-size analysis and ground penetrating radar (GPR) to examine linear dunes in the northwestern Simpson Desert (Fig. 1), describing their response to a Late Quaternary change in the course of the Todd River and also changes in the prevailing wind orientation. It builds on earlier and current work examining Late Quaternary palaeoflooding undertaken nearby on the Todd River by Bourke (1998; in prep.) and to a broader study of Late Quaternary changes in aeolian, fluvial and lacustrine deposits northwest of Alice Springs by English *et al*. (2001). Importantly, our paper addresses problems associated with differentiating the role of climate change, catastrophic flooding and aeolian-dune damming in the modification of dunefields and the avulsion of river channels in central Australia. It specifically illustrates major changes in dune alignment resulting from relocated river flows and altered palaeowind directions.

## LOCATION

### Physiography and Vegetation

The study site is located approximately 150 km southeast of Alice Springs in the northwest corner of the Simpson Desert (Fig. 1). The landscape varies from low but rugged bedrock ridges to low-lying dune-covered desert basins. Near the most easterly extent of the MacDonnell Ranges the Rodinga Range and Train Hills define an east-west syncline, known as Camel Flat basin. They cut across the strike of sand ridges enclosing a relatively small field (~1200 $km^2$) of north- to northwest-orientated linear dunes (Fig. 2). Throughout the basin these well-vegetated dunes are asymmetric with steeper eastern faces, a morphology noted throughout much of the Simpson Desert by Mabbutt *et al.* (1969), Folk (1971) and Nanson *et al.* (1992b, 1995).

In the past, flows from the Todd River entered the eastern side of Camel Flat basin through Wallaby Gap, a natural watergap in the Train Hills, before exiting through the comparable Camel Gap in the Rodinga Range that bounds the southern margin of the basin (Fig. 2). The land surface

generally slopes southwards and the main flow system through the basin ran in a southeasterly direction for 25 km between the two gaps. This palaeofloodplain is relatively straight and featureless with a gradient of around 0.0014 and a width of 1-3 km. A smaller arm from the main system bifurcates immediately south of Wallaby Gap, disappearing into the dunefield about 10 km due south (Fig. 2). A number of other palaeoflow systems entered the far eastern end of the basin near the present Todd River (Fig. 2), but they are not investigated here. The main palaeofloodplain and its distributary south of Wallaby Gap define a marked east-west change in the character of the dunes of the basin. Those on the floor of the eastern part of the basin are relatively small, closely spaced are lighter coloured, courser textured, and have a northwest orientation. They formed on the floodplain since it ceased to be fluvially active. In contrast, dunes in the western part of the basin are larger, more widely spaced, fine textured, dark red in colour and are oriented more to the north (Figs. 3 and 6). Vegetation on the smaller eastern dunes consists of bluebush, canegrass, bibiscus, mulla mulla, cassia and acacia on the dunes with ironwood and saltbush in the swales. The larger, more widely spaced dunes in the western part of the basin support a relatively simple vegetation consisting mostly of spinifex and desert oak. In both areas of the basin the dunes curve westward upwind of the Train Hills before accumulating their greatest sand volumes in the form of ramping-style obstruction and echo dunes on the foot slopes of the range (Figs 4a and 7). The still-visible palaeofloodplain is distinguished by an absence of dunes and it harbours dense groves of gidgee and saltbush vegetation. Small source-bordering dunes line parts of its northeastern boundary, and along its southwestern boundary linear dunes have encroached onto its surface (Fig. 4b). Clearly the floodplain has been much more extensive in the past, for alluvium underlies most of the area demarcated by smaller dunes on the floor of the eastern part of the basin.

**Climate and wind regime**

The Simpson Desert is classified as a hot persistently dry desert, BWh in the Köppen system. The semi-arid climate becomes increasingly arid southward from Alice Springs into the Simpson Desert. This is partially because of a mild orographic effect around the study area but is mostly due to the declining influence of Australia's northern monsoon. The basin receives 285 mm of precipitation annually but this drops to ~190 mm southward away from the ranges, with mean annual evaporation rates measured at Alice Springs in the order of 3070 mm (Bureau of Meteorology, 2003). While there are no temperature data for Camel Flat, variations seasonally and diurnally can be extreme, with the highest maximum and lowest minimum temperatures at Alice Springs (100 km to the northwest) and Finke (125 km to the south; Fig. 1) yielding two-station averages of 46.8°C and -5.7°C for January and July, respectively. Similarly, there are no

wind data for Camel Flat basin but the dominant wind vector at the field site between Alice Springs and Finke is almost certainly from the southeast (Fig. 5). Averaging 3.00 p.m. wind speeds between Finke and Alice Springs shows them predominantly from the southeast sector, highest in February at 15.6 km/hr, and lowest in May/June at 12.7 km/hr (Bureau of Meteorology, 2003).

## FIELD AND LABORATORY METHODOLOGIES

Aeolian dunes and interdunes were instrument surveyed roughly perpendicular to their linear orientation using a Leica total station. Holes were augered by hand at crests on these transverse profiles and at selected distances along the length of a number of dunes. The palaeofloodplains were also augered by hand. Sediment was collected from all auger holes at 1 m intervals for grain size analysis and colour determination using a Munsell Colour Chart. Grain size analyses were undertaken on these samples in the laboratory using a Malvern Mastersizer 2000 laser system. TL samples were collected at roughly 1 m intervals beginning at 1.5 m from the surface in order to minimise the risk of contamination from bioturbation in the upper profile. OSL samples were collected at night using a sand auger. All sampling sites were located with a Garmin GPS 12 XL and their locations are recorded in Table 3.

Ground penetrating radar (GPR) profiles across two dunes were collected using a Pulse Ekko PE 100 with 100 MHz antennae. Surveys were oriented perpendicular to the dune crest with antennae spaced 1 m apart and oriented perpendicular to the survey line with a step size of 0.25 m between measurements and a stack of 32 measurements at each point. Minimum processing, dewow, and an AGC gain have been applied to retain the integrity of the data. Topography along the profiles was surveyed with measurements every 5 m and at breaks of slope. Topographic corrections were performed using Pulse Ekko software. A velocity of 0.15 m.n $s^{-1}$ has been calculated from CMP surveys conducted along the dune crest, this velocity is consistent with published velocities for dry sand (McCann *et al*, 1988; Davis and Annan, 1989).

### TL Laboratory Procedure

The outer exposed layer of each sample was removed and under filtered light conditions and utilised in the determination of the combined (U + Th) alpha activity, potassium and sample moisture content. Following fined crushing the sample alpha activity was determined using thick source alpha counting (TSAC). Samples were sealed in and counted after a three-week period to allow the uranium and thorium decay chains to re-establish. A minimum of 1000 counts was

accumulated in each case thus contributing a counting uncertainty level of 3.2% at 1 standard deviation. The sample potassium content was measured by means of atomic absorption spectrometry. In the final sample annual radiation flux computation an assumption was made for the small contribution made by the presence of rubidium and the cosmic radiation contribution was calculated assuming a half sample depth using the equations given by Aitken (1985). The final radiation flux level was corrected for the modifying effect of present day sample moisture content.

The unexposed portion of each sample was carefully wet sieved to obtain the 90 – 125 μm grain size fraction. This was treated in dilute (8% w/w) HCl, etched in HF (40% w/w) to remove unwanted crystalline grains and finally subjected to heavy liquid separation in sodium polytungstate to remove undesirable heavy minerals which might contribute unwanted TL. The sample so prepared has been shown to consist of almost pure quartz grains.

The prepared quartz sample was divided into two portions one of which was spread in a monolayer in a Petrie tray and placed beneath an ultraviolet lamp (Philips MLU 300W) for a minimum of 24 hours thus simulating the sun's TL resetting action during sediment transport. Fourteen sample aliquots of this and the unreset quartz, each comprising of approximately 5 mg, were deposited using a volumetric method. Any variation between these aliquots was later corrected using a second TL glow normalisation procedure.

Sample aliquots containing laboratory reset quartz grains were serially and incrementally irradiated in the laboratory using a calibrated 90Sr plaque radiation source. The TL thus induced was measured using a Littlemore TL reader fitted with an EMI QB9636 photomultiplier in combination with a Corning 7-57 blue transmission filter. A regenerated TL growth curve was thus prepared and plotted for each sample. The mean natural TL output as determined from eight aliquots was fitted to this curve and thus the radiation dose, accumulated since deposition (palaeodose), was determined.

As a check for possible change in TL sensitivity due to laboratory procedure a series of radiation doses were added to the remaining six natural sample aliquots. Following TL measurement these values were plotted upon the regenerated TL growth curve with respect to the mean natural value. If there has been no change in TL sensitivity these plotted values should coincide with the regenerated curve. By this means the radiation dose absorbed by the sample, since deposition, was computed which, when divided by the annual radiation dose, results in the depositional age of the sample. Detailed results are provided in table 1. Full details of this procedure are given by Nanson *et al.* (1991) and Shepherd and Price (1990).

**OSL Laboratory Procedure**

OSL analyses were undertaken on small aliquots (~100 grains) of 90-125 μm quartz, prepared in the standard manner (e.g., Aitken, 1998), using the modified SAR protocol of Olley *et al*, (in press(a)). This protocol incorporates an 'infrared wash' prior to each green-light stimulation, effectively removing any contribution by contaminant feldspars to the (green-light) OSL signal. For samples (Site 3, 1.5m), (Site 3, 3.5m) and (Site 16, 2.0m), no over-dispersion of the De distributions is evident, therefore burial ages were determined using the central age model of Galbraith *et al*, (1999). Samples (#2,1.0m) and (#2,1.9m) had over-dispersed De distributions (Table 2), suggesting incomplete bleaching prior to deposition. Olley *et al.*, (1998; 1999; in press(a)) have shown that for young, partially bleached material, the most accurate burial dose estimate is provided by the lowest measured Des. Accordingly, the minimum age model (Galbraith and Laslett, 1993; Galbraith *et al*, 1999) has been used to determine burial doses for samples (Site 2,1.0m) and (Site 2,1.6m).

Lithogenic radionuclide activity concentrations were determined from measurements of U, Th and K concentrations using neutron activation analysis of dried and ground bulk samples. Dose rates have been calculated based on the assumption of secular equilibrium in the $^{238}$U and $^{232}$Th chains, using the conversion factors of Stokes *et al*. (2003). Cosmic dose rates were calculated from Prescott and Hutton (1994). Beta-attenuation factors were taken from Mejdahl (1979). Assumed long-term water content of 7 ± 2.5 % has been used to adjust dry dose rates.

Prescott and Hutton (1995) and Olley *et al*. (1996) have shown that disequilibrium in the $^{232}$Th chain is rare in Australian terrestrial samples, however, especially in fluvial environments, disequilibrium in the $^{238}$U chain is common. Although this assumption may cause an underestimation of the dose rate, it has little effect on the final ages in this case, due to the overwhelming contribution of $^{40}$K to the dose rate (mean of five samples = 69%) and the minor contribution from the $^{238}$U chain (mean of five samples = 6.3%, see Table 2).

## SEDIMENTARY CHARACTER AND CHRONOLOGY OF THE DUNES

All the field sites described below are summarised and located as grid references in Table 3.

**Western Camel Flat basin**

Two sites were examined here. Site 15 is located on a 12 m high dune 5 km south of Johnsons Bore Gap in the Train Hills in the field of larger dunes about 14 km west of their boundary with the adjacent smaller eastern dunes (Fig. 6a). These larger dunes have steeper

eastern sides and in places dune crests are semi-active with small blowouts, superimposed dunes and wind ripples. They consist of dark red sand (10R 4/8) that is moderately well sorted and positively skewed, fining with depth. TL analyses gave ages of 73.9 +/- 5.5 ka at 9.1 m, 54.8 +/- 2.8 ka at 8.0 m and 38.9 +/- 2.0 ka at 6.0 m, the basal sample yielding the oldest age obtained for a dune in the Camel Flat basin.

Site 14 is located immediately south of Johnsons Bore Gap on a large ~14-15 m high echo dune 5.5 km north of Site 15 and 80 m from the base of the Train Hills (Fig. 6a). At this site winds, predominantly from the south, have been aerodynamically deformed upwind of the hills (Hollands, 2002). Composite echo dunes have developed here, partially infilling the swales that characterise the linear dunes immediately south. Dunes crests up to 14-16 m high top large volumes of sand that accumulated here because their gradual northward passage under the prevailing wind is blocked by the range. A 10 m deep auger hole exposed uniform fine red sand (10R 4/8) throughout, similar to Site 15 to the south, with the mean grain size and percent silt/clay ranging from 190 μm and 6.61% at 1 m to 170 μm and 13.65% at 9 m depth. A downward fining trend in dune texture was also found by Folk (1971) for dunes in this area. TL analyses obtained dates of 14.4+/-1.1 ka at 4.5 m and 47.3+/-3.7 ka at 9.5 m depth.

**Eastern Camel Flat basin**

The eastern basin shows a complex pattern of dune chronology and development, some dunes having formed on abandoned floodplains and others in slightly elevated positions against the ranges. As in the western basin, large dunes to the north, close to the Train Hills, curve to the west in response to aerodynamic conditions starting several kilometres upwind of the hills (Figs 2 and 4a) (Hollands, 2002). Ramped onto the foothills, these dunes contain fine sand distinctly red in colour, comparable to dunes in western basin. In contrast, dunes on the alluvial floor of the eastern basin are significantly smaller than the ramping dunes or those in the western basin. A significant indicator of their sediment origin is their lighter yellow-red colour and coarser texture, appearing to consist largely of aeolian-reworked fluvial sand.

***Ramping dunes***

Site 1 is the highest dune on the Train Range foothills to be sampled and the dunes here appear to be either superimposed upon a large volume of previously accumulated aeolian sand, or to have accumulated onto a gently sloping pediment south of the range (Figs 4a and 7). Dip angles into the basin from the base of Train Hills taken from seismic surveys by Oaks (1983) are around $6^{o}$, suggesting the latter, however, augering to depths of 8 m in the dune crest and 3 m in the swale indicates at least 11 m of aeolian sand has accumulated at Site 1. Field surveying showed these

dunes to be up to 13 m high, about twice the height of those to the south on the floor of the eastern basin. Swale stratigraphy consists of sandy cracking clays down to about 1 m and relatively clean aeolian sand below that. The Site 1 dune consists of uniform red (2.5YR 4.5/8) fine clean sand (6.39% silt/clay) at the crest with a mean grain size of 148 μm, grading to a slightly darker red (2.5YR 4/8) clayey fine sand (39.18 silt/clay) with a mean grain size of 98 μm at 8 m, moderately well sorted and positively skewed throughout. Folk (1971) also noticed fining-with-depth for dunes between Alice Springs and Finke. As elsewhere, the increase in fines down the profile suggests pedogenesis in the lower part of the dune and/or the flushing of fines downward through the profile over time. No carbonates are present, and TL ages obtained gave 4.9 +/- 0.5 ka at 2.5 m and 28.2 +/-2.0 ka at 7.5 m depth.

Site 4 is located on an ~8 m high crest superimposed on an echo dune 2 km west of Site 1 and ~50 m from the base of Train Hills (Fig. 4a). This location also shows substantial accumulation of aeolian sediment within the dune and adjacent swale. Augering penetrated 12 m but did not reach the base of the dune and revealed red sand throughout (2.5YR 4.5/8), but with mean grain size and percentage fines changing from 152 μm and 8.95% at 1 m to 111 μm and 32.54% silt/clay at 10 m. There is a possible palaeosol at 8 m where silt and clay peak at 46.91%. The texture shows moderately well sorted and positively skewed sediment throughout. TL ages obtained were 6.2 +/-0.4 ka at 2.5 m and 64.8 +/-5.6 ka at 10.5 m, the latter being the oldest dune TL age obtained in the eastern part of the basin.

***Dunes and Alluvium on the Basin Floor***

The eastern part of the basin reveals something of the character of dunes derived from alluvium underlying much of the basin floor and still visible in restricted extent as a dune-free palaeofloodplain corridor between Wallaby and Camel Gaps (Fig. 2). In contrast to the dune sediment of reddish fine sand, the alluvium consists of yellowish medium to coarse sand and even gravel, the light colour presumably resulting from of the removal of iron coatings during fluvial transport.

Site 2 is located on Camel Creek about 800 m from where it exits the Train Hills (Fig. 4a) This small 7.5 $km^2$ bedrock catchment is subject to local flooding. At the sampling site a narrow floodplain is kept clear of aeolian dunes by periodic overbank flows. The surface consists of sand with scattered boulders up to 30 cm diameter. The stratigraphy here is clearly defined so we believe the site has not been reworked by bioturbation at >0.5 m. The upper 1.2 m of alluvium consists of reworked dune sand (121 μm and 24% fines) similar to that at aeolian Sites 1 and 4. At 1.2 m there is a charcoal horizon on a former surface, below which the sediment is similar but slightly coarser (mean 144 μm and 23% fines). An OSL sample in the upper unit at 1 m and gave an age of 3.6+/-0.3 ka, and another at 1.6 m in the unit below and gave an age of 4.0+/-0.3 ka. Below 2 m the undated section consisted of well-rounded medium to large pebbles with some light coloured (5YR 5/6) fluvial sand. Dates from the two uppermost units suggest

significant local late Holocene flooding carrying pebbles and boulders from the bedrock catchment, probably partly suspended in high-density flows resulting from incorporated locally eroded dune sand.

Site 3 is located on the southern branch of the palaeofloodplain, 4 km south of Wallaby Gap (Fig. 4a). The upper nearly 1 m of sediment appears to be mostly aeolian; it is red (2.5YR 4/6) with the fine texture of dune sand. Below 1 m is clearly alluvial with medium to fine sand mixed with 13% coarse sand and granules and a few pebbles, and the silt/clay content is 35%. There is an abrupt change after 2 m where coarse sand and gravels make up 18%, accompanied by a change in colouration to yellow/red (5YR 5/6). At 3 m colouration changes to pink (5YR 7/3), coarse-medium sand and pebbles constitute 26% of material. OSL gave an age of 73 +/- 5.0 ka at 1.5 m, and 64 +/- 6.0 ka at 3.5 m. Site 3 contains the oldest alluvium sampled in the basin, equivalent to the basal age of the oldest dated dune (Site 15) and older than fluvial activity elsewhere in the area noted by Bourke (1998).

At Site 16 the palaeofloodplain was augered to a depth of 3 m. Here the upper 1.2 m consisted of a sheet of red aeolian sand underlain by a dense palaeosol of pedogenic carbonate to 1.7 m. A well defined horizon of fluvial sand to 2.3 m with a mean size of 312 μm and consisting of 24% mud and 23% coarse sand yielded an OSL date of 66+/-6.0 ka at 2.0m. This unit is underlain at 2.8 m with what appeared to be poorly sorted fluvial sand partly indurated with calcite.

At Site 17, about 300 m due north of the palaeochannel, a low fairly continuous 3-5 m high source-bordering dune consists of vertically uniform yellow-red (5YR 5/6) sand with a mean size of 163 μm, 11% mud and <2% coarse sand, that flanks the northeastern edge of the palaeofloodplain. At 3.5 and 5.0 m depth it was TL dated at 10.1 +/- 0.5 and 10.8 +/- 0.8 ka, respectively.

At Site 5, 1.5 km south of the southern edge of the palaeofloodplain corridor (Fig. 6b) a 6 m high dune is composed of yellow/red (5YR 5/6) fine to coarse sand. Here the swales have a surface cover of polished very-coarse sand with a few well-rounded fluvial pebbles. The mean sediment size in the dune grades from 302 μm at the crest to 173 μm at the base, with positive skewness throughout. Light coloured fluvial sand is clearly visible in samples throughout the dune. The major difference between dunes on the basin floor and those ramping northward onto the Train Hills is in their percentage of coarse sand. Sites 1 and 4 have none while Site 5 contains 14.63% at the dune crest and 4.34% at the base, indicating a local fluvial source. As elsewhere in the basin, the percentage of fines progressively increases with depth, in this case from 12.44% silt/clay at 1 m to 30.61% silt/clay at 5 m depth. TL dating yielded ages of 4.6 +/-0.3 ka at 2.5 m and 10.1 +/-0.8 ka at 5.5 m depth. Excavations in the swale reveal 1 m of clayey sand above what

appears to be about 2 m of aeolian sand. A depth of 3 m below the swale surface sees the gradual mixing of aeolian sand with coarser, lighter-coloured fluvial sand.

Sites 12 and 13 are located some 10 km down the palaeofloodplain from Site 5 and also represent dunes encroaching the palaeofloodplain's southern edge (Fig. 4b). Site 12 is located 140 m from the dune terminus where the dune is only ~2.5 m in height. At 1 m depth it consists of red (2.5YR 4/6) sand which is unusual for this alluvial location. But sediment texture is diagnostic of an alluvial origin, consisting of 10% coarse sand giving a positively-skewed sand with a mean size of 235 μm. At 3 m depth, the percentage of coarse sand decreases to 6% with a mean size of 164 μm. A TL age of 4.1 +/- 0.3 ka was obtained at 2.5 m depth, the same level in the dune as the adjacent plain. At 4 m depth the sediment is poorly sorted and dark red (2.5YR 3/6) with 20% coarse sand and granules and a high (43%) silt/clay content, clearly a fluvial deposit later partly indurated with calcium carbonate. At 5 m depth a different fluvial sequence is denoted by an abrupt colour and texture change to a light reddish-brown (5YR 6/4,) sandier sediment consisting of 9% coarse sand and small pebbles and only 16% silt/clay. An auger hole in the swale to the southwest of Site 12 revealed a 1 m veneer of aeolian sand with scattered clay-pan laminations and some granules and pebbles swept in from the adjacent palaeochannel, with dark red (2.5YR 3/6) very clayey sand below 5 m.

Site 13 is located on a very low dune east of Site 12, but approximately 250 m upwind of the dune's most distal extent onto the palaeofloodplain (Fig. 4b). Polished fluvial sediments are mixed in with aeolian sand on the swale surface. The upper 3 m of the dune consists of moderately well sorted, positively skewed red sand (2.5YR 4/6). The percentage of silt/clay increases from 21% at 1 m depth to 29.4% at 3 m. Coarse sand (7.47%) is found only in the first metre of sediment accounting for a mean size of 234 μm that decreases to 164 μm at 3 m. At a depth of 2.5 m a TL age of 9.8 +/- 0.8 ka was obtained about 1 m below the present topographic form of the dune. It probably represents the age of the aeolian sand plain that covers the alluvium both in the swales and under the dunes in this part of the basin. The alluvium at 4 m consists of fine, medium, and coarse sand and pebbles mottled with carbonate. At 5 m depth, a dark red (2.5YR 3/6) alluvium contains a high percentage of fines (41%) mixed with 30.6% coarse sand and granules and contains carbonate. This appears to be the same alluvium as occurs at Site 12 at 4 m depth. At 6 m the alluvium is a lighter red colour (2.5YR 4/6) than above and consists of 27.95% fines mixed with 27.4% coarse sands and granules.

Several dune sites overlying alluvium were also examined on the floor of the eastern basin, upwind of the palaeofloodplain. Sites 6 and 10 represent two locations 6.5 km apart along the same dune (Fig. 6b) and were examined in order to see if such dunes show evidence of having prograded downwind. Site 6, some 5 km south of the palaeochannel, consists of uniform

yellow/red (5YR 5/6) sand from 1 to 5 m with a gradual increase grain size from 8.57% silt/clay and a mean size of 269 μm (9.8% coarse sand) at the crest to 16.2% fines and a mean size of 198 μm (4.82% coarse sand) with small carbonate nodules at 5 m where the dune is 15.2 +/- 1.1 ka or slightly older in age. At 6 m there is an abrupt change to yellow/red (5YR 4/6) alluvium with 13.92% poorly sorted coarse sands and granules, 45% silt/clay and an increase in the size of carbonate nodules. Upwind some 6.5 km along the same dune, Site 10 is composed of darker red sediment (5YR 5/8) and yielded a much older TL age of 35.7 +/-2.7 ka at 4.5 m depth. This is the oldest age obtained for any dune on the eastern floor of Camel Flat basin. Grain size declines from the crest where the mean size is 180 μm with 0.3% coarse sand and 10.33% silt/clay to near the base at 5 m where there is no coarse sand and the mean size is 156 μm with 35.4% silt/clay. The size distribution is positively skewed throughout but changes to negatively skewed in a distinctive yellow/red (5YR 5/6) alluvium at 6 m depth due to the presence of coarse sand and granules (10.4 %). On the basis of age, stratigraphy and sedimentology, the two sites sampled along this dune are of very different giving the impression of a feature that becomes significantly younger downwind. Ages at 4.5 m depth at both sites range from ~36 ka in the south to ~15 ka in the north, suggesting a dune migration rate northwards of 0.31 $ma^{-1}$.

Sites 7, 8 and 9 are also spaced along the crest of a single linear dune, in this case over a distance of 3 km and immediately east of the dune discussed above (Fig. 6b). Site 7 consists of uniform yellow/red (5YR 5/6) sand, similar to Site 5 and 6, with an increasing proportion of fine sediment from the crest at 1 m (mean size 312μm, coarse sand 12.53%, silt/clay 6.07%) towards the aeolian base at 6 m (mean size 192 μm, coarse sand 3.5%, silt/clay 22.03%). Crestal sediment has around 10% polished sand gains probably blown in from adjacent swales, but not enough to produce a significant colour difference. At 7 m the profile appears to be alluvium containing 3.5% of very coarse sand. TL ages of 4.4 +/-0.4 ka and 10.8 +/-0.9 ka were obtained at 2.5 m and 4.5 m, respectively.

Site 8 is located approximately 1.5 km upwind of Site 7 (Fig. 6b). The crest at 1 m is red (2.5YR 5/8) with a mean grain size of 284 μm, 5.63% silt/clay and 8.12% coarse sand. At 4 m the colour darkens slightly (2.5YR 4/8), the mean size declines to 138 μm with silt/clay content increasing to 28.64% and coarse sand declining to just 0.11%. TL dating provided ages of 9.6 +/-0.8 ka at 2.5 m and 20.8 +/-2.0 ka at 4.5 m depth. A GPR profile conducted across this dune revealed a palaeosol reflector at ~4 m that mimics the dune surface but with the dune crest now offset some 20 m to the east (Fig. 8a). The upper part of the dune appears to have been reworked eastward with the addition of lighter coloured and coarser textured sand than that beneath the palaeosol.

Site 9 is located farthest upwind on this particular dune (Fig. 6b). Here the crest consists of red sand (2.5YR 4/8) with a mean size of 186 μm (9.51% silt/clay and 0.33% coarse sand; significantly less coarse sand compared to the crests at Sites 5, 6, 7 and 8 nearer the palaeofloodplain corridor). At 5 m depth, fines increase to 26.41% with no coarse sand. At 6 m there is an abrupt change to a yellow/red (5YR 5/6) alluvial unit consisting of 32% coarse sand and granules. TL ages of 13.5 +/-1.2 ka at 2.5 m and 23.7 +/- 1.9 ka at 4.5 m, represent aeolian activity with the basal fluvial unit dating at 24.9 +/-4.9 ka. This suggests aeolian processes commenced at this location shortly after cessation of fluvial activity. A GPR profile reveals a palaeosol reflector at ~4 m depth and movement of the dune crest to the east by about 40-50 m (Fig. 8b), somewhat farther than that at Site 8. The ages of dune material above and below the palaeosol are also similar to those at Site 8. As at Sites 6 and 10, this sequence of ages along the dune suggests progressive dune growth to the northwest, with ages at 2.5 m depth changing from ~13.5 ka in the south to ~4.4 ka in the north, suggesting a migration rate of 0.33 $ma^{-1}$, with basal ages at 4.5 m depth changing from ~24 ka to ~11 ka and suggesting a migration rate of 0.23 $ma^{-1}$. Results of analyses in the two separate linear suggest they both extended northwards onto the basin alluvium towards the remaining palaeofloodplain from about 35 ka to 4 ka at a rate of about 0.23 to 0.33 $ma^{-1}$ with and accompanying eastward accretion of about 0.003 $ma^{-1}$. There is no evidence of dune deformation or a significant hiatus in dune progradation as a result of flows onto this floodplain since ~25 ka, although it is quite probable that the present palaeofloodplain corridor experiences local flooding with runoff from the Train Hills.

A plot of dune chronology against distance from the southern margin of the presently visible palaeofloodplain in Camel Flat basin (Fig. 10) suggests that the eastern dunefield has migrated northwards, relatively slowly for the first 4km (from12 to 8 km in Fig. 10) between about 35 and 10 ka, and then relatively rapidly since 10 ka over the remaining 8 km.

## DISCUSSION

Our initial interpretation was that the palaeofloodplain through Camel Flat basin was formed in the Pleistocene by catastrophic overflows from the Todd River rather than being the sole or primary course of the river prior to the LGM. However, there is nothing to suggest that the present water gap on the Todd River where it passes through the Train Hills is a more likely position for the main channel than is Wallaby Gap. Indeed the river has to deviate abruptly eastward at Mosquito Bore to reach its present position through the Train Hills (Bourke, 1998). The description and chronology of dunes and alluvium presented here suggest that the Todd River

passed through Camel Flat basin between about 75 and 25 ka and that it subsequently entirely or largely abandoned this course by avulsing to its present position. This interpretation is supported by evidence of very extensive alluviation of the eastern part of the basin until 25 ka, and almost none since then. Although Bourke (1998) obtained an OSL date of ~10 ka on the palaeofloodplain 6 km downstream from Wallaby Gap (Fig. 4a), her sample was from just 0.8 m in depth. Such a shallow deposit could be the product of local runoff from the Train Hills, similar to the samples we OSL dated at ~3.6 and ~4 ka from Site 2 on Camel Creek. Furthermore, the ages of alluvium dated along the present Todd River by Bourke (1998) are complementary to those obtained here for alluvium in Camel Flat basin. They indicate very large flows close to the present course of the Todd River over the past ~14 ka (Bourke, 1998: pers. Comm., 2004), but so far no evidence of earlier flows at that location. Dunes on the palaeofloodplain surface of the basin show no sign of any significant flood deformation, however, their more rapid northward progression since ~10 ka (Fig. 10) may be due to reduced flooding and increased aridity since then. Whether such Late Pleistocene flooding was locally derived from the ranges, or due to overflows from the Todd River near Mosquito Bore, will not be clear until dating of the palaeosystem in between is undertaken. However, the presence of a 10-11 ka source-bordering dune along the palaeofloodplain (Site 17, Fig. 4b) is supporting evidence for some flow through the system until then. In terms of the broader regional picture, the alluvium within the basin does not correspond in age to the period of substantial flooding from 20 ka onwards recognised by English *et al*. (2001) at Lake Lewis. However some flooding probably did persist through Camel Flat until about 10 ka. In summary therefore, evidence at present suggests that Camel Flat was actually the primary course of the Todd River prior to the LGM and not just a Pleistocene overflow system for a river that occupied essentially its present position.

Major avulsions of the Todd River in the MacDonnell Ranges have probably been caused, at least in part, by aeolian dunes obstructing narrow water gaps, forcing the river to find alternative passages. Bourke (1998, pp118) recognised the probability of channel avulsion of the Todd River when she wrote: " The terminal floodout has been positioned in three different locations during the late Pleistocene. Moving from east to west they are the mosquito bore distributary [wallaby gap], the rodinga gap distributary and the modern floodout." Satellite images and airphotos show numerous palaeofloodplains through the ranges and dunefields of this area. Indeed the results obtained here, and subsequent discussion, identify the difficulty of separating the impacts of climate change, catastrophic flooding and aeolian damming as possible causes of landscape change for the region as a whole.

The oldest dunes in the eastern Camel Flat basin are ramped up on the foot-slopes of the Train Hills above the palaeofloodplain. Their basal ages range between 65 ka and 28 ka, but it is

very likely they are older beyond the 10 m reach of our hand auger. The large dunes on the floor of the western basin appear to have been stable for at least as long, one yielding a near basal age of 74 ka. In combination these older dates suggest a component of the dunefield of the northwestern Simpson Desert has been present in the Camel Flat basin for most of the Late Pleistocene. However, as suggested by Nanson *et al.* (1992a, 1995), unconsolidated dunes are vulnerable to periodic aeolian reworking or fluvial erosion, so even relatively old ages are almost certainly not indicative of the age of initial dune development in central Australia. Elsewhere, Australian dunes have returned luminescence ages of between 200-300 ka (Readhead, 1984; Wasson, 1986; Nanson *et al.*, 1988, 1992b; Bowler *et al*., 2001), with Bowler (1982) suggesting from palaeomagnetic evidence that the onset of dune activity in the Mallee region of southern Australia was around 700 ka. Also using palaeomagnetic data, Chen and Barton (1991) suggested the onset of severe aridity in central Australia occurred at about 1 Ma. However, such aridity was clearly interspersed with episodes of pronounced wetness (Nanson et al., 1992b; Bowler et al., 2001). English *et al*. (1991) found that wet conditions prevailed for much of the Early and Middle Pleistocene at Lake Lewis, ~150 km northwest of Alice Springs, changing to more arid conditions during the Late Pleistocene before becoming exceptionally arid at around 23-21 ka. As a result, the combination of pronounced variations in widespread aridity along with fluvial aeolian interactions near the ranges have almost certainly resulted in a very complex picture of channel change in the vicinity of the MacDonnell Ranges.

The oldest aeolian TL date obtained from the base of a dune over alluvium on the floor of the eastern basin is ~36 ka (Site 10), just 3 km from the foot-slope of the Rodinga Range in the south. This compares to dates of ~25 ka from the alluvium and an overlying dune nearby (Site 9). From here the dunes become progressively younger northwards towards the remnant palaeofloodplain where they are about 4 ka. It appears that extensive fluvial activity in the basin ceased at or just before just before the LGM and that since then dunes have migrated progressively northwards at a rate of about 0.25-0.35 $ma^{-1}$ over the alluvial surface. It is possible that Camel Flat basin was isolated from the Todd River by the development of aeolian dunes at Wallaby Gap or farther upstream during that period of pronounced dune activity in the region (English *et al*., 2001). This would have forced the river to breach the Train Hills farther eastward at its present position, abandoning its course through the basin.

The linear dunes in the western part of Camel Flat basin are oriented broadly northwards but the younger dunes in the eastern part are oriented some $20^0$ more towards the west (Fig. 3). The eastern dunefield appears to reflect a post LGM southeastward shift in the prevailing wind direction, with the western dunes having been orientated earlier by winds more from the south. Contrasting dune patterns across the Camel Flat basin are evidence that anticyclonic wind patterns

associated with the continental whorl of dunes were modified during the Late Pleistocene at about the time of the LGM. Mabbutt (1967) suggested that the anticyclonic core strengthened and expanded during this period. Wasson (1986) proposed latitudinal shifts and strengthening of the anticyclonic core. Nanson *et al.* (1995) specified a 1.0-1.5$^{o}$ northward latitudinal shift in the axis of the wind system at Finke during the last glacial, then a return to its present position during the Holocene. A southward shift in the central Australian wind-whorl after the LGM could account for the change in dune orientation in Camel Flat basin (Fig. 9). A location of linear dunes in the whorl with the same orientation as the smaller eastern dunes in Camel Flat basin exist north of the Harts Range on the northern planes. This is approximately 160 km or 1.5$^{o}$ north of Camel Flat basin (Fig. 9). As the eastern dunes are roughly aligned to modern winds and are mostly post LGM in age, it is suggested that the anticyclonic wind patterns was positioned about 160 km north earlier in the Late Pleistocene at the time of dune formation in the western part of Camel Flat basin. This is remarkably similar to the estimated position of the Late Pleistocene wind whorl about 100-150 km farther north at the time regional dunes were oriented near Finke (Nanson *et al.,* 1995).

Dunes in Camel Flat basin have steep eastern faces and low angled western plinths suggesting they have been subjected to dominant winds from their western flank after their initial formation. GPR stratigraphic profiles of a linear dune in the eastern basin reveal an eastward shift of its crest by 20-50 m with TL dates in the upper half of these suggesting it occurred around 10-14 ka. Whether this has been the product of lee-side or windward-side accretion (Nanson *et al*., 1992a) is difficult to gauge since the dunes show no internal sedimentary structures in their GPR record, probably as a result of biogenic processes during such slow lateral accumulation.

## CONCLUSIONS

Although the dunefields of Australia appear as a relatively continuous whorl about the centre of the continent, Brookfield (1970) suggested that the pattern maybe a coincidence of wind trajectories rather than a single synoptic anticyclonic whorl. This study demonstrates that in places the dunefields consist of spatially discrete components that are different in character and age. The linear dunes of the northwest Simpson Desert are obviously deformed by local aerodynamic conditions near the ranges (Hollands, 2002). However, the linear dunes in the eastern part of Camel Flat basin well away from the ranges also illustrate a distinctive alignment because they are younger than those for the remainder of the regional dunefield. While much of the regional dunefield southeast of Alice Springs has retained a south to north orientation, apparently imposed

earlier in the Quaternary, those formed after the LGM in Camel Flat basin on the abandoned floodplains of the Todd River appear to be a response to winds more from the southwest.

On the basis of morphology, alignment, chronology, sedimentology and colour, the dunes at Camel Flat can be separated into three geomorphic zones. First, ramping dunes of fine red aeolian sand have accumulated on the foot-slopes of the ranges and are larger, with a much greater sand volume per unit length than any other dunes in the basin. It is apparent that northward sand transport during the Late Quaternary has piled sand up against the obstructing ranges since at least 65 ka. Second, the floor of the western part of the basin consists of large (~12 m high) widely spaced dunes of fine red aeolian sand that yielded a near basal age of ~74 ka, not dissimilar to dunes ramped onto the footslopes. Third, the eastern part of the basin consists of a palaeofloodplain that dates between 73-64 ka and 25 ka. Overlying this alluvium are aeolian dunes with basal ages of 25 to 4 ka that are progressively younger northwards due to linear-dune progradation that averaged about 0.25-0.35 $ma^{-1}$ but was most rapid after about 10 ka They are formed of lightly coloured relatively coarse sand derived from the underlying alluvium, and are oriented ~$20^{o}$ farther to the west due to a post LGM change in wind direction. This wind shift appears to be the result of a 160 km or $1.5^{o}$ southward movement of the whorl of winds that orientated most of the Pleistocene-age dunes in this part of the Simpson Desert. This is similar to the findings of Nanson *et al.* (1995) for changes in wind Late Quaternary direction at Finke on dunes also influenced by fluvial activity.

Clearly, the eastern extremity of the MacDonnell Ranges in central Australia is an area that contains a detailed but complex story of Late Quaternary fluvial and aeolian interaction. Consequently, a challenge remains in distinguishing or interrelating the roles played by climate change, catastrophic flooding and aeolian damming in modifying this landscape.

**REFERENCES**

Aitken, M.J., 1985. Thermoluminescence Dating. Academic Press, London.

Aitken, M.J., 1998 An introduction to Optical Dating: The Dating of Quaternary Sediments by the Use of Photon-Stimulated Luminescence. Oxford University Press, Oxford.

Bourke, M.C., 1998. Fluvial Geomorphology and Palaeofloods in Central Australia. PhD Thesis. ANU, Canberra.

Bowler, J.M., 1982. Aridity in the late Tertiary and Quaternary of Australia. In: Barker, W.R., Greenslade, P.J.M., (Eds.), Evolution of the Flora and Fauna of Arid Australia. Peacock Press, Adelaide, pp. 35-46.

Bowler, J.M., Wyrwoll, K.H., and Lu, Y., 2001. Variations of the northwest Australian summer monsoon over the last 300,000 years: the palaeohydrological record of the Gregory (Mulan) Lakes system. Quaternary International. 83-85, 63-80.

Brookfield, M., 1970. Dune trends and wind regime in central Australia. Zeitschrift fur Geomorphologie Supplementband 10, 121-153.

Bureau of Meteorology, 2003. Home Page. http://www.bom.gov.au

Chen, X.Y., Barton, C.E., 1991. Onset of aridity and dune-building in central Australia: sedimentological and magnetostratigraphic evidence from Lake Amadeus. Palaeogeography, Palaeoclimatology, Palaeoecology 84, 55-73.

Davis, J.L., and Annan, A.P., 1989. Ground penetrating radar for high resolution mapping of soil and rock stratigraphy. Geophysical Prospecting 37, 531-551.

English, P., Spooner, N.A., Chappell, J., Questiaux, N.G., Hill, N.G., 2001. Lake Lewis basin, central Australia: Environmental evolution and OSL chronology. Quaternary International 83-85, 81-101.

Folk, R.L., 1971. Longitudinal dunes of the northwestern edge of the Simpson Desert, Northern Territory, Australia, 1. Geomorphology and grain size relationships. Sedimentology 16, 5-54.

Galbraith, R.F., Laslett, G.M., 1993. Statistical models for mixed fission track ages. Nuclear Tracks and Radiation Measurements 21, 459-470.

Galbraith, R.F., Roberts, R.G., Laslett, G.M., Yoshida, H. Olley, J.M., 1999. Optical dating of single and multiple grains of quartz from Jinmium rock shelter, northern Australia: Part I, experimental design and statistical models. Archaeometry 41, 339-364.

Goudie, A.S., Wells, G.L., 1995. The nature, distribution and formation of pans in arid zones. Earth-science Reviews 38, 1-69.

Hollands, C.B., 2002. Aeolian dune morphology, chronology and evolution at Camel Flat in the northwest Simpson Desert, Australia. Unpublished BSc (Hons) Thesis, University of Wollongong, Wollongong.

King, D., 1960. The sand ridge deserts of South Australia and related aeolian landforms of the Quaternary arid cycles. Transactions of the Royal Society of South Australia 83, 99-109.

Mabbutt, J.A., 1967. Denudation chronology in central Australia. Structure, climate, and landform inheritance in the Alice Springs area. In: Jennings, J.N., & Mabbutt J.A., (Eds), Landform Studies from Australia and New Guinea, ANU Press, Canberra pp. 144-181.

Mabbutt, J.A., Wooding, R.A., Jennings, J.N., 1969. The asymmetry of Australian desert sand ridges. Australian Journal of Science 32, 159-160.

Mejdahl, V., 1979. Thermoluminescence dating: beta-dose attenuation in quartz grains. Archaeometry 21, 61-72.

McCann, D.M., Jackson, P.D., and Fenning, P.J., 1988. Comparison of the seismic and ground probing radar methods in geological surveying. Proc. Inst. Elec. Eng., 135, part F, No 4, 380-390.

Nanson, G.C., Price, D.M., Short, S.A., Young, R.W., Jones, B.J., 1991. Comparative Uranium-Thorium and Thermoluminescence Dating of weathered Quaternary alluvium in the Tropics of Northern Australia. Quaternary Research 35, 347-366.

Nanson, G.C., Chen, X.Y., Price, D.M., 1992a. Lateral migration, thermoluminescence chronology and colour variation of longitudinal dunes near Birdsville in the Simpson Desert, Central Australia. Earth Surface Processes and Landforms 17, 807-819.

Nanson, G.C., Price, D.M., Short, S.A., 1992b. The wetting and drying of Australia over the last 300ka. Geology 20, 791-794.

Nanson, G.C., Chen, X.Y., Price, D.M., 1995. Aeolian and fluvial evidence of changing climate and wind patterns during the past 100ka in the western Simpson Desert, Australia. Palaeogeography, Palaeoclimatology, Palaeoecology 113, 87-102.

Nanson, G.C., Young, R.W., Price, D.M., Rust, B.R., 1988. Stratigraphy, sedimentology and late Quaternary chronology of the Channel Country of western Queensland. In: Warner R.F. (Ed), Fluvial geomorphology of Australia, Academic Press, Sydney, pp. 151-175

Oaks, R.Q., 1983. Petroleum prospects and geology- northern Amadeus Basin. Magellan Petroleum Australia Ltd, Brisbane.

Olley, J.M., Murray, A., Roberts, R.G., 1996. The effects of disequilibria in the uranium and thorium decay chains on burial dose rates in fluvial sediments. Quaternary Science Reviews 15, 751-760.

Olley, J.M., Caitcheon, G., Murray, A., 1998. The distribution of apparent dose as determined by optically stimulated luminescence in small aliquots of fluvial quartz: implications for dating young sediments. Quaternary Science Reviews 17, 1033-1040.

Olley, J.M., Caitcheon, G.G., Roberts, R.G., 1999. The origin of dose distributions in fluvial sediments, and the prospect of dating single grains of quartz from fluvial deposits using optically stimulated luminescence. Radiation Measurements 30, 207-217.

Olley, J.M., Pietsch, T., Roberts, R.G., (in press a) Optical dating of Holocene sediments from a variety of geomorphic settings using single grains of quartz. Geomorphology.

Olley, J.M., De Deckker, P., Roberts, R.G., Fifield, L.K., Hancock G. (in press b) Optical dating of deep-sea sediments using single grains of quartz: a comparison with radiocarbon. Sedimentary Geology

Prescott, J.R., Hutton, J.T., 1994. Cosmic ray contributions to dose rates for luminescence and ESR dating: large depths and long-term time variations. Radiation Measurements 23, 497-500.

Prescott, J.R., Hutton, J.T., 1995. Environmental dose rates and radioactive disequilibrium from some Australian luminescence dating sites. Quaternary Science Reviews 14, 439-448.

Readhead, M.L., 1984. Thermoluminescence dating of some Australian sedimentary deposits. PhD Thesis. Australian National University, Canberra.

Shepherd, M.J., Price, D.M., 1990. Thermoluminescence dating of late Quaternary dune sand, Manawata/Horowhenua area, New Zealand: a comparison with $^{14}C$ age determinations. New Zealand Journal of Geology and Geophysics 33, 535-539.

Stokes, S., Ingram, S., Aitken, M.J., Sirocko, F., Anderson, R., Leuschner, D., 2003. Alternative chronologies for Late Quaternary (Last Interglacial-Holocene) deep sea sediment via optical dating of silt-size quartz. Quaternary Science Reviews 22, 925-941.

Wasson, R.J., Fitchett, K., Mackey, B., Hyde, R., 1988. Large-scale patterns of dune type, spacing and orientation in the Australian continental dunefield. Australian Geographer 19, 89-104.

Wasson, R.J., 1986. Geomorphology and Quaternary history of the Australian continental dunefields. Geographical Review of Japan 59, 55-67.

## ACKNOWLEDGEMENTS

We greatly appreciate the support of Locky and Paddy Weir who provided access to their property, Allambi, and to Martin Klien and Tim Cohen for their willing assistance in the field.

**FIGURE CAPTIONS**

**Figure 1**. Map of Simpson Desert region with insert locating study area shown in Figure 2.

**Figure 2.** Camel Flat with inserts showing site locations in detail. Site A is shown in Figure 4A, Site B in Figure 4B, Site C in Figure 6A and Site D in Figure 6B. The palaeofloodplain of the Todd River is shown passing through Wallaby Gap and Camel Flat Gap.

**Figure 3. A.** Large, widely spaced dunes in the vicinity of Site 15 in the western part of Camel Flat basin. **B.** Smaller, more closely spaced dunes in the eastern part of Camel Flat basin in the vicinity of Site 5. **C.** The surveyed cross-sections at Sites 5 and 15, with TL dates included. Both these sites are located in Figure 6.

**Figure 4. A.** Sites 1, 2 and 4 located near the Train Hills, Sites 3 and Site MBR3 (Bourke, 1998) located on the palaeofloodplain. **B.** Sites 12 and 13 are located furthest downwind on dunes extending onto the floodplain. Site 16 located on the palaeochannel, with Site 17 on an adjacent source-bordering dune. See Figure 2 for locations.

**Figure 5. A.** Wind rose data at Alice Springs and **B.** at Finke, both plotted showing average dune orientations in the Camel Flat basin.

**Figure 6. A.** Sites 14 and 15 in the western part of Camel Flat basin. **B.** Sites 5-11 in the eastern part of Camel Flat basin, south of the palaeofloodplain. See Figure 2 for locations.

**Figure 7.** Surveyed profile at Site 1 indicating TL ages. Note the ramping of dune material onto the base of the Train Hills.

**Figure 8. A.** Site 8 and **B.** Site 9 showing GPR profiles and TL ages revealing older dune cores at each site (below the palaeosol reflectors), the upper part of each dune having accreted eastwards.

**Figure 9**. Diagrammatic representation of wind whorl associated with the orientation of linear dunes in Camel Flat basin (greater detail of the Camel Flat location on the right). The eastern dunefield is orientated to the modern wind with the western dunefield indicating the former prevailing wind from the south. See the text for an explanation of a ~160 km northward migration of the wind whorl since alignment of the western dunefield.

**Figure 10.** Upper and lower dune chronology plotted against distance from the presently visible aeolian-alluvial southern boundary of the palaeofloodplain. The trend suggests northward migration of these linear dunes.

**Table 1.** Thermoluminescence data of sites in the Camel Flat basin.

**Table 2.** Dose estimates, dispersion parameters, dose rates (total and U derived) and calculated OSL ages for sites in the Camel Flat basin.

**Table 3.** Sedimentary characteristics of sites in the Camel Flat basin. Grid coordinates also included.

**Table 1**
**Thermoluminescence Data**

| Site & Sample Depth (m) | Sample Number | Temp. Plateau Region (ºC) | Palaeodose (Grays) | K Content (% by AES) | Moisture Content (% by weight) | Specific Activity (Bq/kg U+Th) | Cosmic Contribution (µGy/yr assumed) | Annual Radiation Dose (µGy/yr) | TL Age (ka) |
|---|---|---|---|---|---|---|---|---|---|
| 1/2.5 | W3060 | 275-500 | 14.4+/-1.3 | 1.65+/-0.05 | 1.5+/-3 | 52.2+/-1.2 | 144+/-25 | 2962+/-61 | 4.9+/-0.5 |
| 1/7.5 | W3061 | 300-500 | 88.5+/-6.1 | 1.70+/-0.05 | 2.0+/-3 | 61.9+/-1.4 | 95+/-25 | 3143+/-62 | 28.2+/-2.0 |
| 4/2.5 | W3062 | 275-500 | 16.6+/-1.1 | 1.65+/-0.05 | 2.4+/-3 | 39.9+/-1.3 | 144+/-25 | 2686+/-61 | 6.2+/-0.4 |
| 4/10.5 | W3063 | 300-500 | 158+/-13 | 1.45+/-0.05 | 1.0+/-3 | 39.9+/-4.3 | 72+/-25 | 2443+/-62 | 64.8+/-3.6 |
| 5/2.5 | W3064 | 275-500 | 18.8+/-1.4 | 2.50+/-0.05 | 1.0+/-3 | 60.7+/-1.9 | 144+/-25 | 4058+/-65 | 4.6+/-0.3 |
| 5/5.5 | W3065 | 275-500 | 39.4+/-2.9 | 2.45+/-0.05 | 1.7+/-3 | 57.4+/-1.3 | 123+/-25 | 3884+/-61 | 10.1+/-0.8 |
| 6/4.5 | W3077 | 300-500 | 54.6+/4.0 | 2.10+/-0.05 | 2.6+/-3 | 63.0+/-1.9 | 123+/-25 | 3589+/-64 | 15.2+/-1.1 |
| 7/2.5 | W3067 | 275-500 | 13.0+/-1.1 | 2.00+/-.05 | 0.6+/-3 | 33.8+/-1.1 | 144+/-25 | 2992+/-65 | 4.4+/-0.4 |
| 7/4.5 | W3068 | 275-500 | 34.2+/-2.9 | 2.00+/-0.05 | 0.9+/-3 | 44.1+/-1.4 | 123+/-25 | 3170+/-62 | 10.8+/-0.9 |
| 8/2.5 | W3069 | 300-500 | 26.7+/-2.3 | 1.65+/-0.05 | 2.0+/-3 | 44.3+/-1.4 | 144+/-25 | 2787+/-61 | 9.6+/-0.8 |
| 8/4.5 | W3070 | 300-500 | 64.8+/-6.1 | 1.80+/-0.05 | 2.8+/-3 | 55.2+/-1.7 | 123+/-25 | 3114+/-63 | 20.8+/-2.0 |
| 9/2.5 | W3071 | 275-500 | 37.3+/-3.3 | 1.55+/-0.05 | 2.6+/-3 | 49.3+/-1.4 | 144+/-25 | 2762+/-61 | 13.5+/-1.2 |
| 9/4.5 | W3072 | 300-500 | 73.6+/-5.7 | 1.80+/-0.05 | 3.4+/-3 | 56.1+/-1.8 | 123+/-25 | 3112+/-63 | 23.7+/-1.9 |
| 9/6.5 | W3073 | 275-500 | 94.3+/-6.9 | 2.50+/-0.05 | 1.1+/-3 | 49.7+/4.4 | 102+/-25 | 3791+/-62 | 24.9+/4.9 |
| 10/4.5 | W3078 | 300-500 | 102+/-7 | 1.65+/-0.05 | 2.5+/-3 | 49.9+/-1.4 | 123+/-25 | 2863+/-61 | 35.7+/-2.7 |
| 12/2.5 | W3075 | 275-500 | 12.8+/-1.0 | 1.70+/-0.05 | 1.1+/-3 | 55.5+/-1.5 | 144+/-25 | 3096+/-62 | 4.1+/-0.3 |
| 14/4.5 | W3074 | 275-500 | 33.6+/-2.4 | 1.45+/-0.05 | 2.6+/-3 | 33.9+/-4.0 | 123+/-25 | 2329+/-59 | 14.4+/-1.1 |
| 14/9.5 | W3079 | 300-500 | 105+/-8 | 1.50+/-0.05 | 2.9+/-3 | 27.9+/-0.9 | 80+/-25 | 2214+/-39 | 47.3+/-3.7 |
| 15/6.0 | W3507 | 300-500 | 89.2+/-3.9 | 1.35+/-0.05 | 0.4+/-3 | 35.1+/-1.2 | 110+/-25 | 2294+/-62 | 38.9+/-2.0 |
| 15/8.0 | W3508 | 275-450 | 124+/-5 | 1.30+/-0.05 | 0.6+/-3 | 37.9+/-1.2 | 87+/-25 | 2268+/-62 | 54.8+/-2.8 |
| 15/9.1 | W3509 | 300-500 | 179+/-12 | 1.40+/-0.05 | 0.5+/-3 | 40.1+/-1.3 | 81+/-25 | 2417+/-62 | 73.9+/-5.5 |
| 17/3.5 | W3510 | 275-500 | 37.9+/-1.7 | 2.10+/-0.05 | 0.8+/-3 | 67.4+/-1.9 | 135+/-25 | 3765+/-65 | 10.1+/-0.5 |
| 17/5.0 | W3511 | 275-450 | 41.0+/-2.9 | 2.10+/-0.05 | 0.6+/-3 | 69.7+/-2.2 | 116+/-25 | 3805+/-67 | 10.8+/-0.8 |

CAMEL FLAT, TL DATING NOTES

(1) These samples were analysed by means of the combined regenerative and additive method using the 90 - 125 micrometer quartz grain size fraction.

(2) All samples displayed excellent TL characteristics which suggests that effective TL resetting prior to final deposition. These samples exhibited long temperature plateaux and TL growthcurves with r-square correlation coefficients approaching unity. In all but a single case, W3079, a second order polynomial solution was applied to the TL growthcurve data. In the case of sample W3079, a third order polynomial provided a better data fit.

(3) The second TL glowcurve characteristics exhibited in all cases proved similar suggesting a similar provenance for each of the samples analysed.

(4) The specific activity of these specimens was measured by means of calibrated thick source alpha counting over a 42mm, scintillation screen. The values shown assume secular equilibrium for both the U and Th decay chains. The uncertainty levels indicated represent one standard deviation.

(5) All samples were analysed at a temperature of 375ºC

(6) Rb Content (ppm assumed) 100+/-25 for all samples

**Table 2**
**Optically Stimulated Luminescence Data**

| Site & Sample Depth | De (Gy) | $\sigma_d$[a] (%) | Dr (Gy/ka) | U Dr[b] (%) | Age (ka) |
|---|---|---|---|---|---|
| 2/1.0m | 4.2 ± 0.3 | 35 | 1.16 ± 0.06 | 4.2 | 3.6 ± 0.3 |
| 2/1.6m | 5.4 ± 0.2 | 58 | 1.34 ± 0.08 | 10.8 | 4.0 ± 0.3 |
| 3/1.5m | 116 ± 4 | 1 | 1.59 ± 0.10 | 7.1 | 73 ± 5 |
| 3/3.5m | 200 ± 11 | 1 | 3.14 ± 0.17 | 1.9 | 64 ± 6 |
| 16/2.0m | 204 ± 8 | 13 | 3.09 ± 0.21 | 7.4 | 66 ± 6 |

CAMEL FLAT, OSL DATING NOTES

[a] The over-dispersion parameter, '$\sigma_d$', is calculated as the relative standard deviation of the single-aliquot De distribution after taking into account the measurement uncertainty for each aliquot, using the central age model of Galbraith *et al*, (1999). If measurement uncertainty were the only source of error in a distribution then $\sigma_d$ would be 0. Olley *et al*, (*in press(b)*) suggest a $\sigma_d$ value < ~20 % to be indicative of uniform bleaching prior to deposition.

[b] Proportion of the dose rate derived from the $^{238}U$ chain, assuming secular equilibrium. By comparison, Olley *et al*, (1996) suggest a typical fluvial sample has about 27 % of its dose rate derived from the $^{238}U$ chain.

**Table 3**

**Sedimentary Characteristics and Map Grid References**

| Depth (m) | Mud % | Sand % | ≥ Coarse sand % | Colour | Mean grain size (μm) |
|---|---|---|---|---|---|
| | | **Site 1 Athernita MP 812148** | | | |
| *2.5* | 15.39 | 88.04 | 0 | 2.5YR 4.5/8 | 132.7 |
| *7.5* | 39.18 | 60.82 | 0 | 2.5YR 4.5/8 | 102.3 |
| | | **Site 2 Athernita MP 806143** | | | |
| *1* | 23.46 | 76.54 | 0 | 2.5YR 4/6 | 121.1 |
| *1.6* | 23.62 | 76.38 | 0 | 2.5YR 4/6 | 144.6 |
| | | **Site 3 Train Hills MP 742113** | | | |
| *1.5* | 8.41 | 73.51 | 18.27 | 5 YR 5/6 | 362 |
| *3.5* | 6.19 | 67.5 | 26.31 | 5 YR 7/3 | 635.2 |
| | | **Site 4 Athernita MP 794144** | | | |
| *2.5* | 10.74 | 89.32 | 0 | 2.5 YR 4.5/8 | 138.6 |
| *8* | 46.91 | 53.09 | 0 | 2.5 YR 4.5/8 | 110.9 |
| | | **Site 5 Athernita MP 799088** | | | |
| *2.5* | 14.07 | 74.69 | 11.24 | 5 YR 5/6 | 276.1 |
| *5.5* | 30.61 | 65.04 | 4.34 | 5 YR 5/6 | 173.2 |
| | | **Site 6 Athernita MP 806062** | | | |
| *4.5* | 8.57 | 86.12 | 5.31 | 5 YR 5/6 | 205.4 |
| | | **Site 7 Athernita MP 828041** | | | |
| *2.5* | 6.29 | 83.26 | 10.45 | 5 YR 5/6 | 280.9 |
| *4.5* | 9.62 | 85.37 | 5.01 | 5 YR 5/6 | 209.1 |
| | | **Site 8 Athernita MP 836028** | | | |
| *2.5* | 12.16 | 81.12 | 6.72 | 2.5 YR 5/8 | 256.4 |
| *4.5* | 28.61 | 71.26 | 0.1 | 2.5 YR 4/8 | 136.8 |
| | | **Site 9 Athernita MP 844015** | | | |
| *2.5* | 13.09 | 89.78 | 0.27 | 2.5 YR 4/8 | 180.6 |
| *4.5* | 25.01 | 74.99 | 0 | 2.5 YR 4/8 | 218.3 |
| *6.5* | 16.4 | 77.24 | 6.36 | 5 YR 5/6 | 357.8 |
| | | **Site 10 Athernita MP 839008** | | | |
| *4.5* | 28.53 | 70.15 | 1.32 | 5 YR 5/8 | 165.9 |
| | | **Site 12 Athernita MP 907073** | | | |
| *2.5* | 4.72 | 79.48 | 8.8 | 2.5 YR 4/6 | 163.7 |
| | | **Site 14 Train Hills MP 559053** | | | |
| *4.5* | 9.48 | 90.22 | 0 | 10R 4/8 | 190.4 |
| *9.5* | 13.65 | 86.35 | 0 | 10R 4/8 | 170.7 |
| | | **Site 15 Train Hills MP 585737** | | | |
| *6* | 7.32 | 91.03 | 1.64 | 10R 4/8 | 189.7 |
| *8* | 9.35 | 88.83 | 1.82 | 10R 4/8 | 195.9 |
| *9.1* | 15.77 | 83.49 | 0.74 | 10R 4/8 | 158 |
| | | **Site 16 Athernita MP 905094** | | | |
| *2.1* | 24.25 | 52.82 | 22.95 | 5 YR 7/3 | 312.2 |
| | | **Site 17 Athernita MP 905096** | | | |
| *3.5* | 10.64 | 88.14 | 1.22 | 5 YR 5/6 | 163.1 |
| *5* | 12.87 | 82.77 | 4.36 | 5 YR 5/6 | 186.8 |

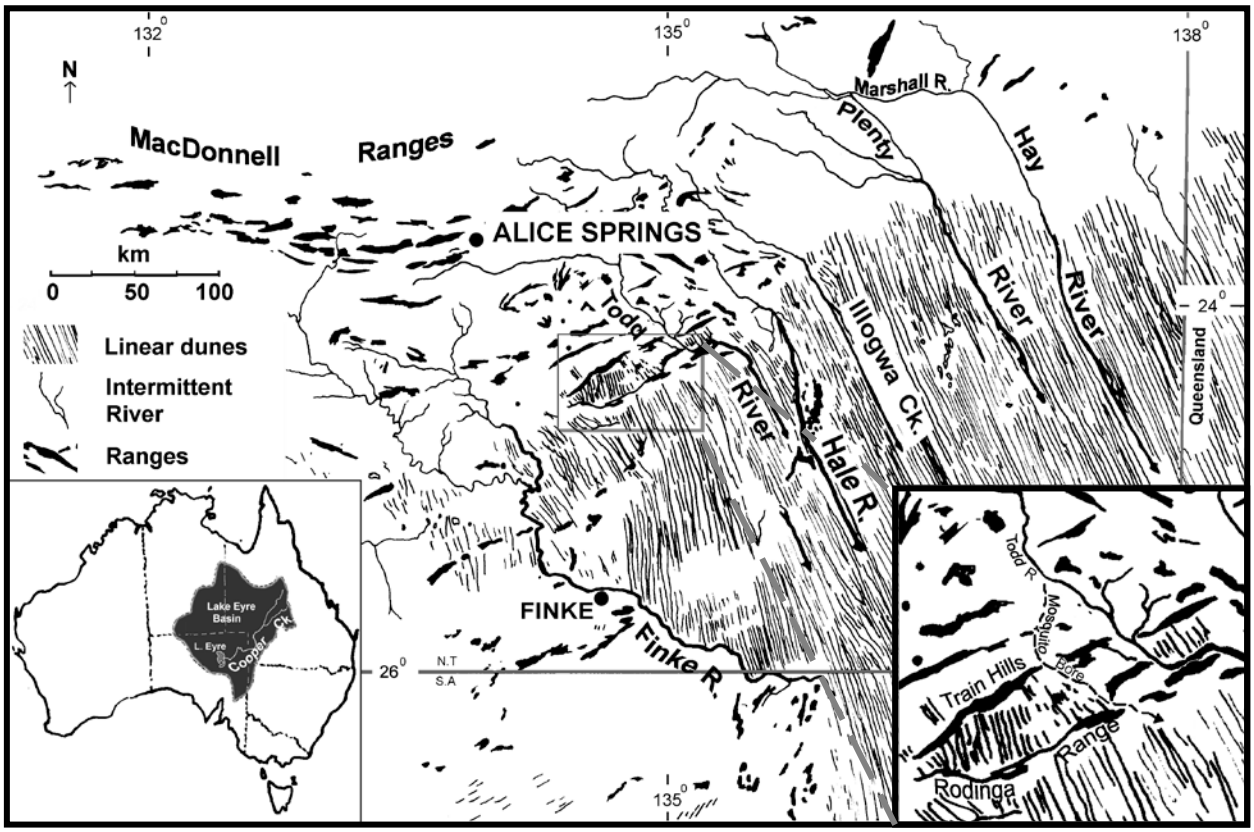


Figure 1

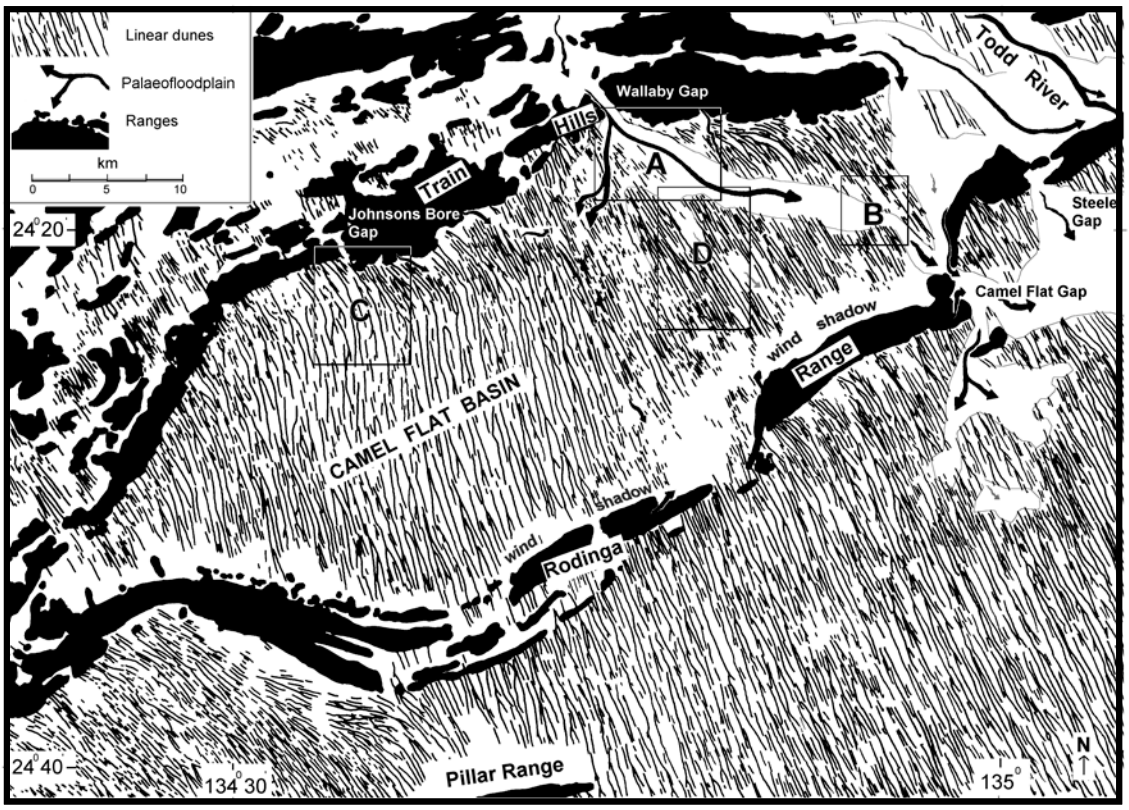


Figure 2

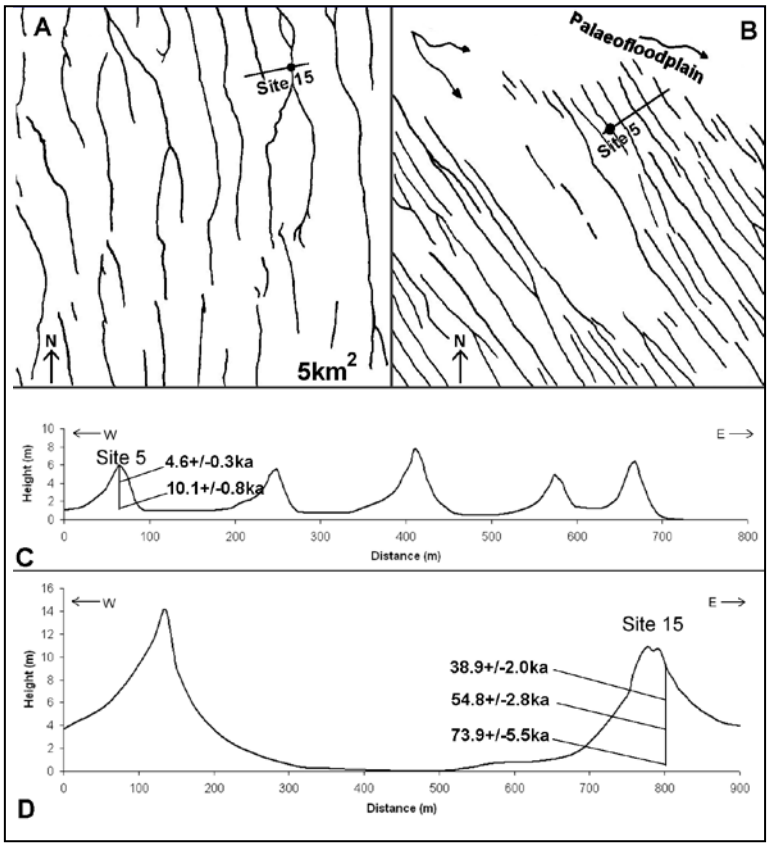


Figure 3

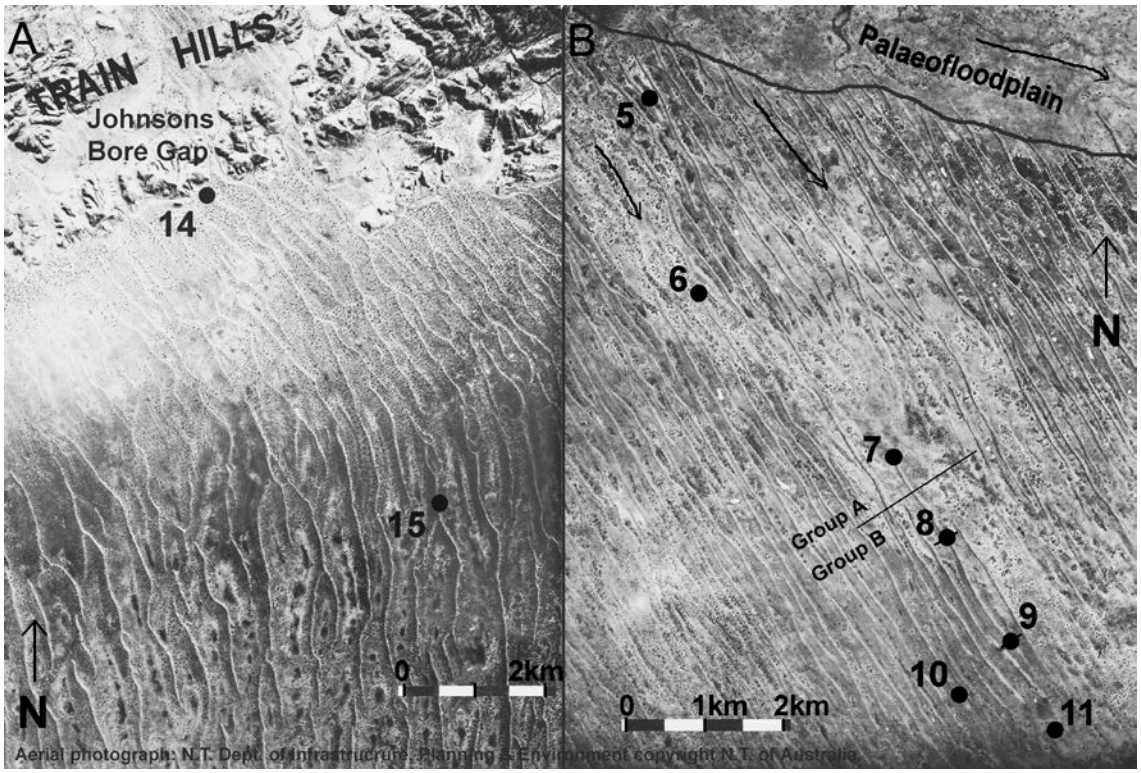


Figure 4

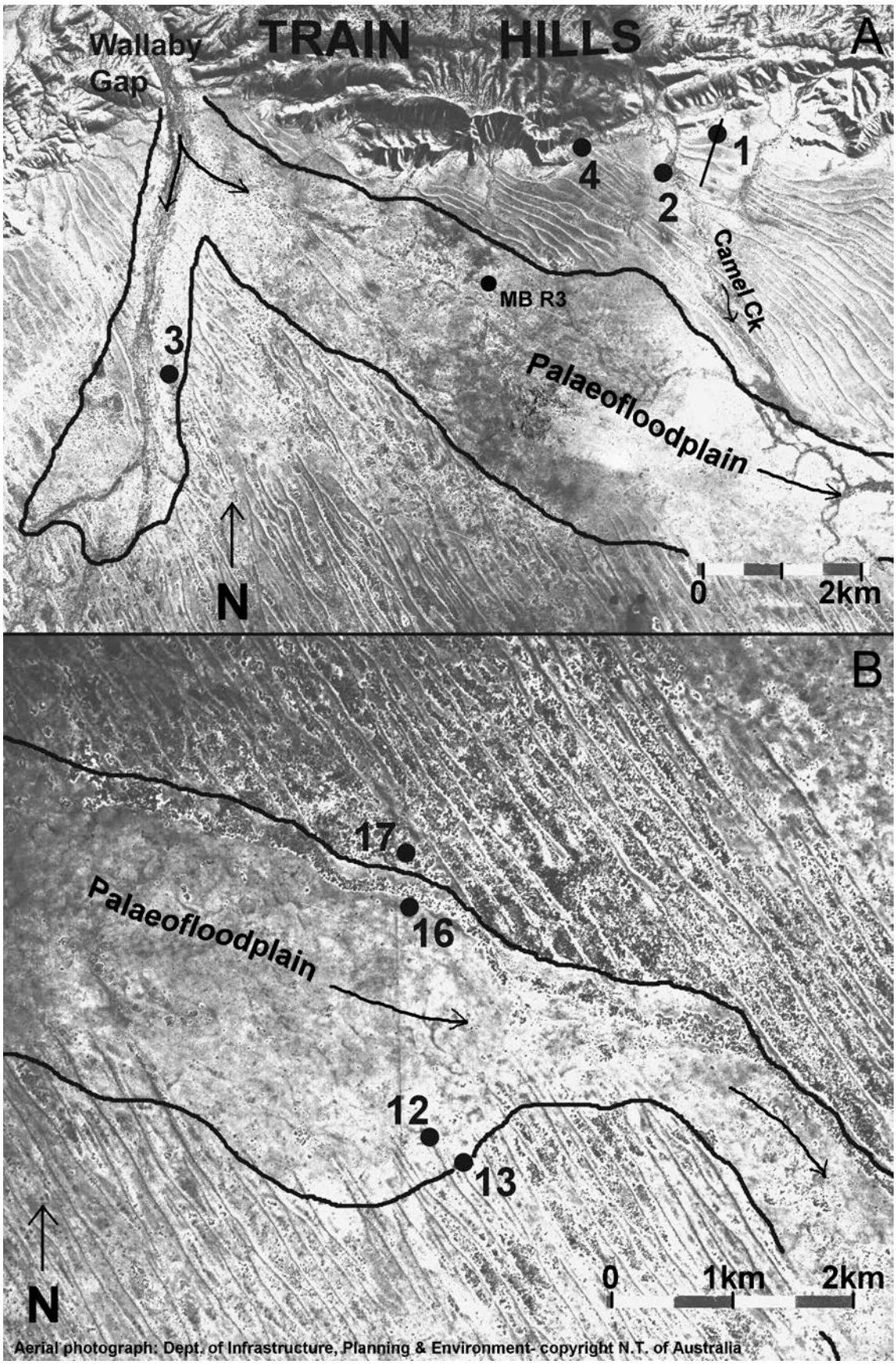
Wallaby Gap
TRAIN HILLS
A
1
2
4
Camel Ck
MB R3
3
Palaeofloodplain
N
0
2km
B
17
16
Palaeofloodplain
12
13
N
0
1km
2km
Aerial photograph: Dept. of Infrastructure, Planning & Environment- copyright N.T. of Australia

Fig 5

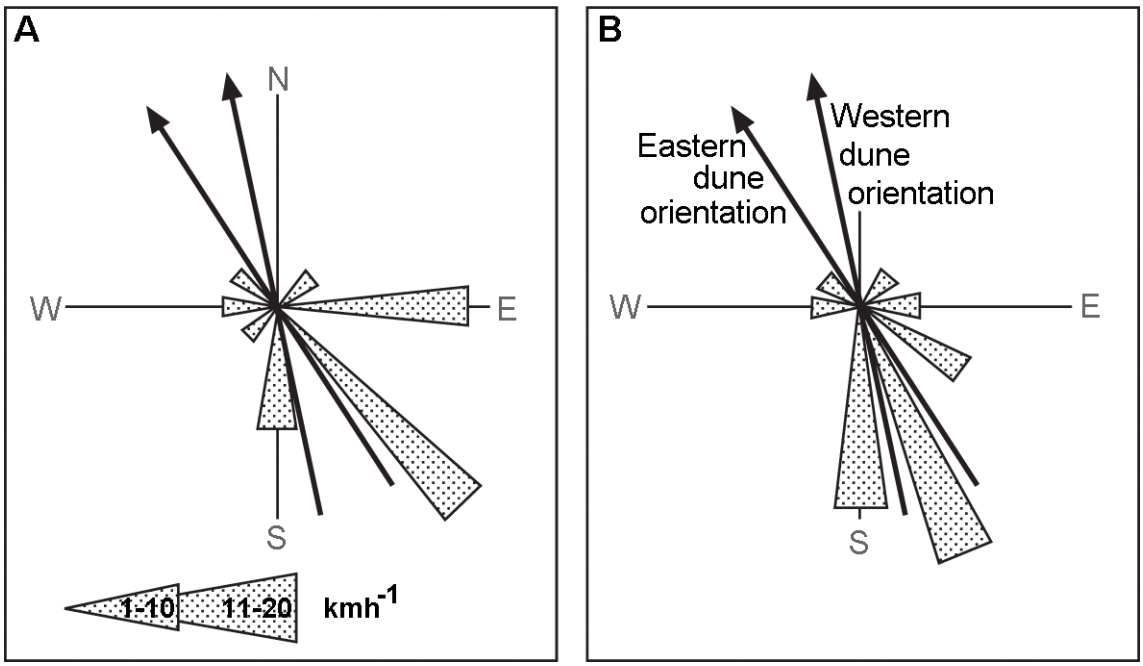


Fig. 6

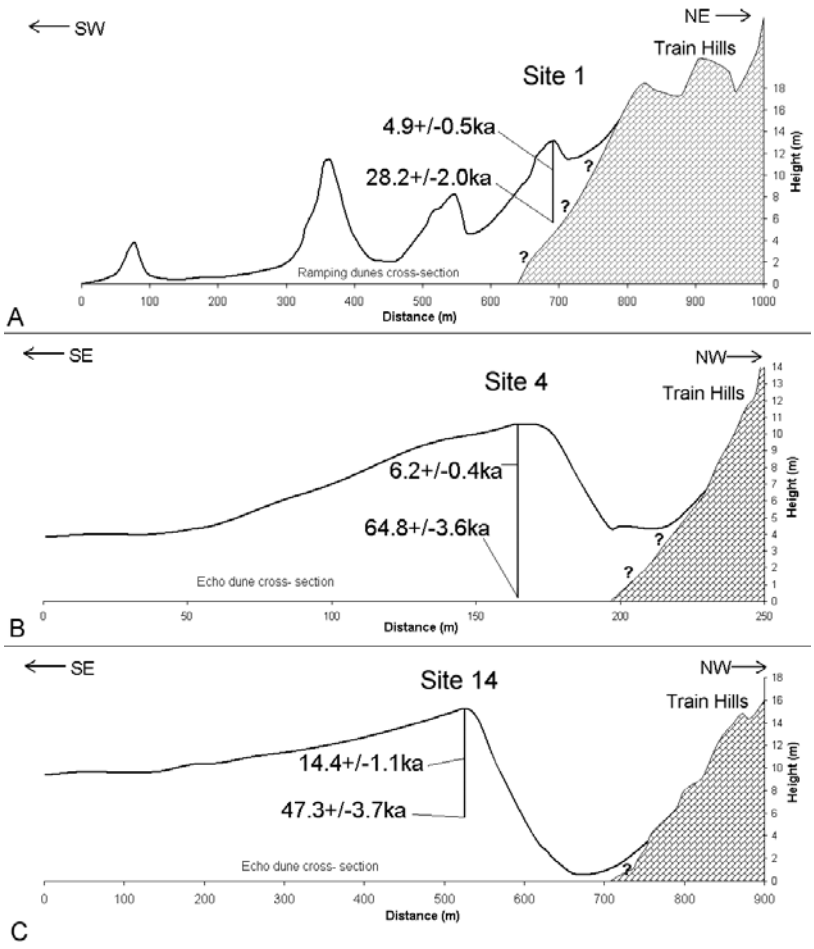


Figure 7

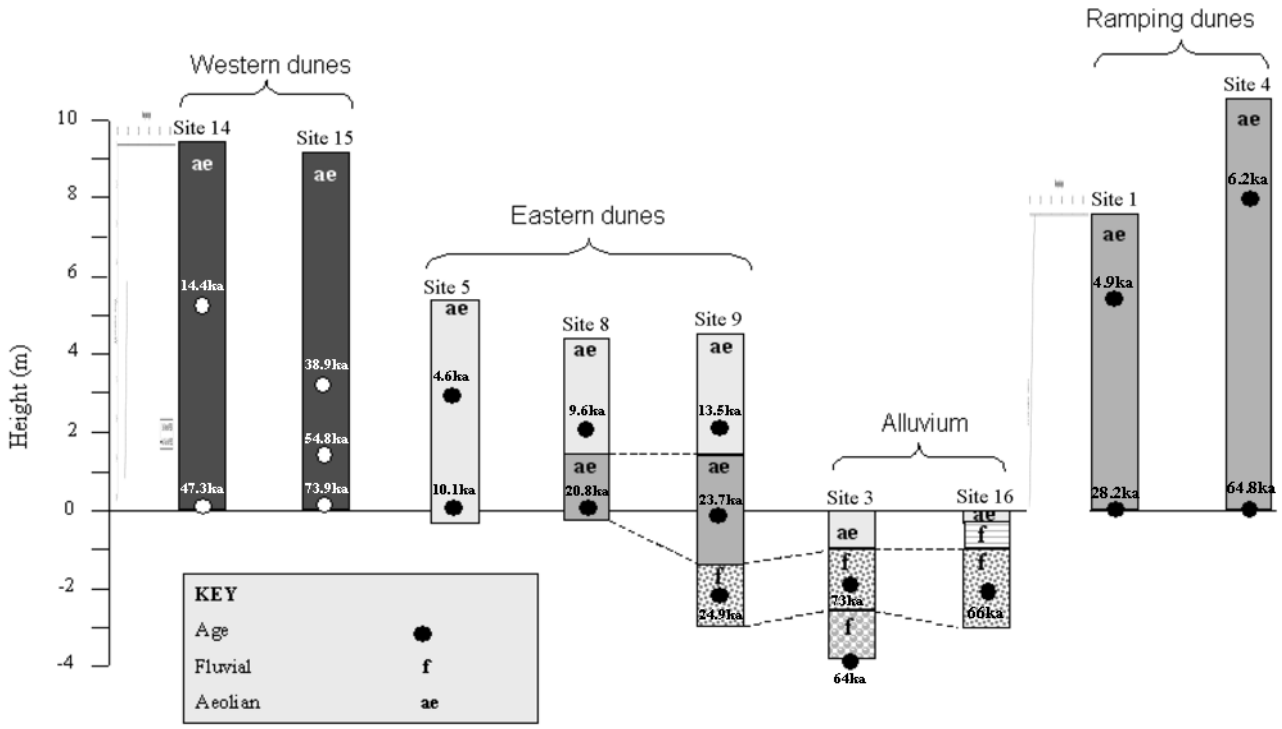
Western dunes
Eastern dunes
Alluvium
Ramping dunes
Site 14
Site 15
Site 5
Site 8
Site 9
Site 3
Site 16
Site 1
Site 4
Height (m)
10
8
6
4
2
0
-2
-4
ae
f
14.4ka
47.3ka
38.9ka
54.8ka
73.9ka
4.6ka
10.1ka
9.6ka
20.8ka
13.5ka
23.7ka
24.9ka
73ka
64ka
66ka
4.9ka
28.2ka
6.2ka
64.8ka
KEY
Age
Fluvial
Aeolian

Figure 8

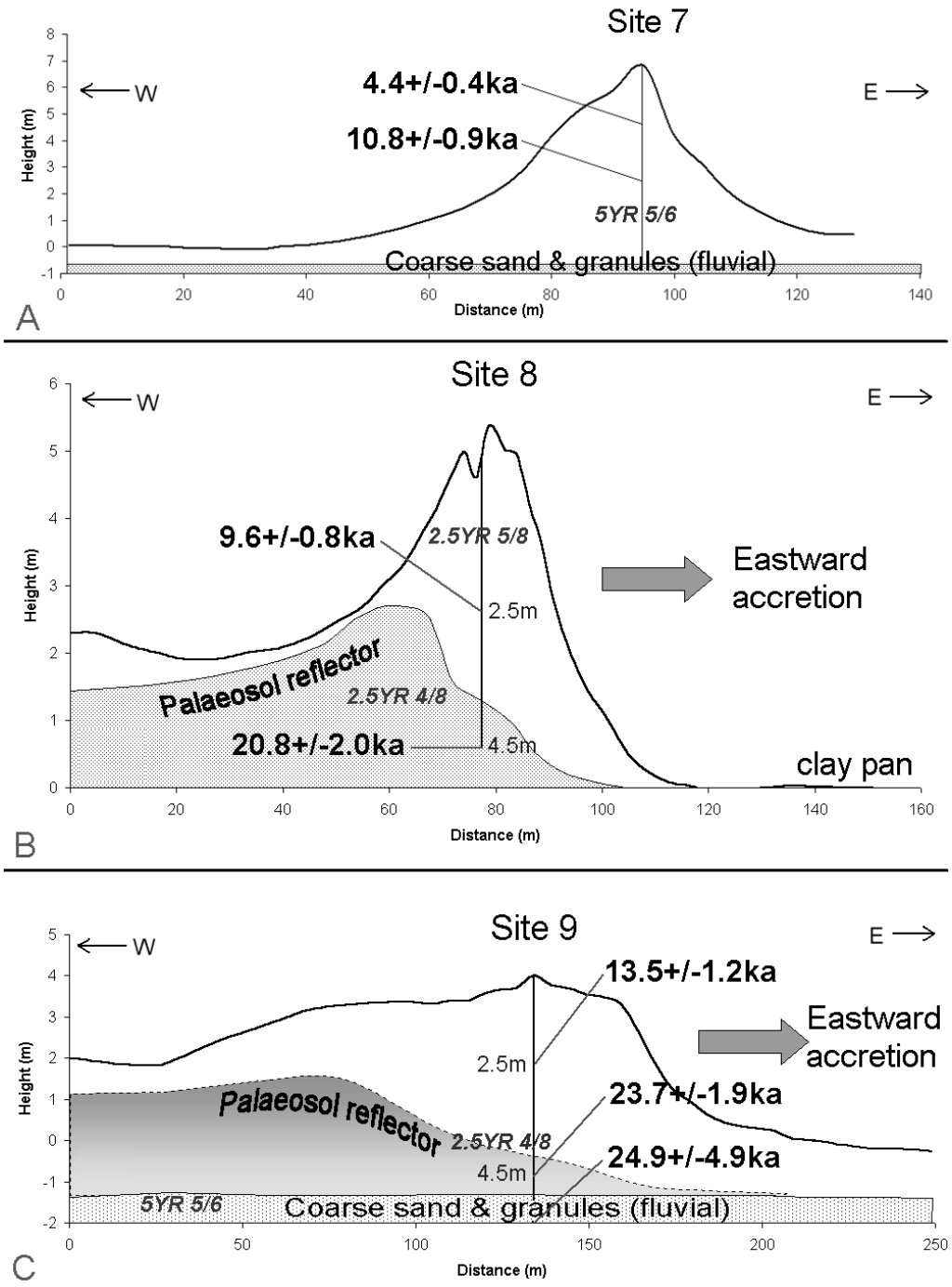
Site 7
W
E
4.4+/-0.4ka
10.8+/-0.9ka
5YR 5/6
Coarse sand & granules (fluvial)
Height (m)
Distance (m)
A
Site 8
W
E
9.6+/-0.8ka
2.5YR 5/8
2.5m
Eastward accretion
Palaeosol reflector
2.5YR 4/8
20.8+/-2.0ka
4.5m
clay pan
Height (m)
Distance (m)
B
Site 9
W
E
13.5+/-1.2ka
Eastward accretion
2.5m
Palaeosol reflector
2.5YR 4/8
23.7+/-1.9ka
24.9+/-4.9ka
4.5m
5YR 5/6
Coarse sand & granules (fluvial)
Height (m)
Distance (m)
C

Figure 9

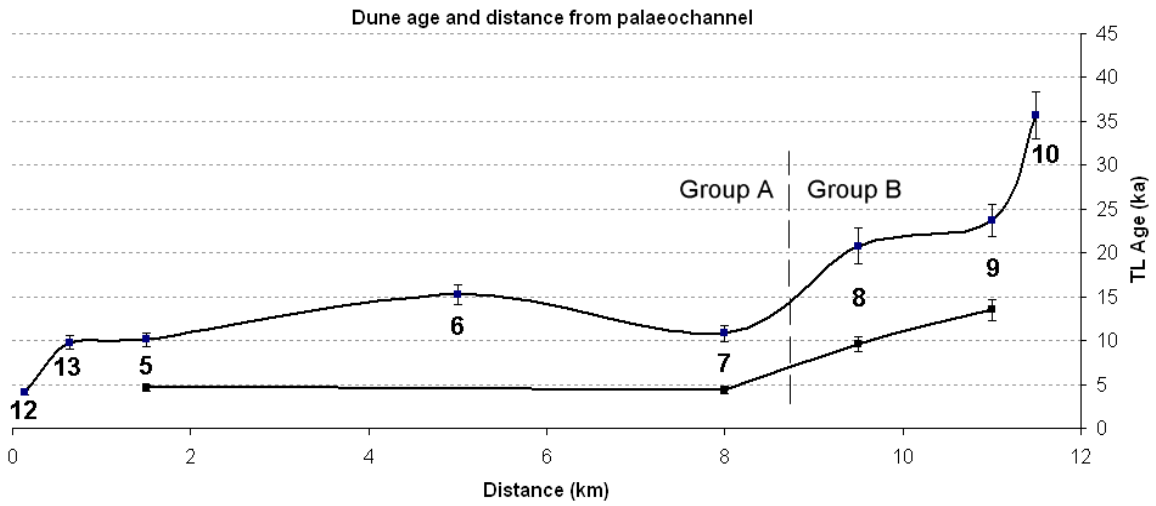


Figure 10

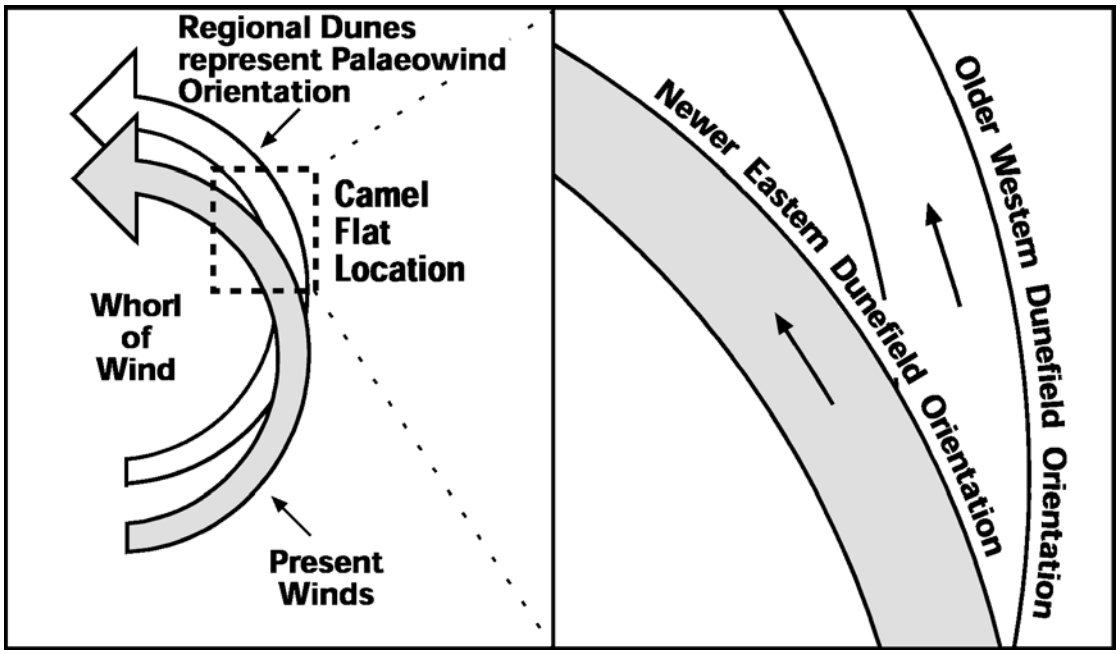


Figure 11